JOURNAL OF MATERIALS SCIENCE 27 (1992) 2599–2605

Suppression of θ″ formation in the SiC whisker-reinforced Al–4 wt% Cu composites

T. S. KIM, T. H. KIM
Department of Metallurgical Engineering, Seoul National University, Seoul, Korea
K. H. OH, H. I. LEE
Materials Engineering Division, Korea Advanced Institute of Science and Technology, Seoul, Korea

Precipitation characteristics in a powder metallurgy (Al–4 wt% Cu)–SiC whisker composite were investigated using transmission electron microscopy, differential scanning calorimetry, and macrohardness measurement. The results of macrohardness measurement show that the peak ageing is significantly retarded in the SiC whisker-reinforced Al–Cu alloys. It is shown that the suppression of θ″ formation plays an important role in the retarded age hardening. The suppression of θ″ formation is attributed to a high density of dislocations due to the difference in the thermal contraction between the whiskers and matrix. Numerical analysis was performed to estimate the misfit strain generated during cooling near the whiskers. The results indicate that a high density of dislocations should be developed by the relief of the misfit strain.

1. Introduction

It has been reported recently [1–5] that the precipitation characteristics of an aluminium metal matrix were significantly altered by the introduction of various reinforcements. An accelerated ageing phenomenon has been reported in the 6061 Al–23 vol % B_4C_p composite [1] and in the 2124 Al–15 wt % SiC_w composite [2]. Subscript p and w denotes particulate and whisker, respectively. It was suggested [1, 2] that a high density of dislocations generated by the differential thermal contraction between the matrix and the reinforcement plays an important role in the accelerated ageing. The suppression of the GP zone formation has been reported in sintered aluminium powder (SAP) type Al–Cu–Si/Al_2O_3 [3] and Al–Cu/Al_2O_3 [4], and in the 6061 Al-δ alumina fibre composite [5]. The most probable cause of such a phenomenon was suggested to be the lack of quenched-in vacancies following the solution treatment, due to the availability of a large number of vacancy sinks at reinforcement–matrix interfaces. However, the precipitation characteristics of the aluminium metal matrix could be affected by other effects. Nutt and Carpenter [6] reported the interfacial segregation of magnesium and the heterogeneous distribution of matrix phases in the 15 vol % SiC whisker-reinforced 2124 aluminium alloy.

In subsequent studies [7, 8] on the SiC whisker-reinforced 7091 and 2024 aluminium alloys, we have clearly found that the control of matrix properties is very important in enhancing the properties of composites. Through differential scanning calorimetry studies we observed the accelerated precipitation of 2024 aluminium alloy and concluded that systematic studies on the precipitation behaviour of aluminium alloy reinforced with SiC whiskers are needed to control the properties of the composites. In this study we investigated the precipitation characteristics of SiC whisker-reinforced Al–Cu alloys processed by P/M techniques. Particular attention was focused on the precipitation behaviour of θ″ and θ′, which play an important role in the matrix strengthening of Al–Cu–SiC whisker composite. The age-hardening behaviour of the processed material was studied using macrohardness measurement, differential scanning calorimetry (DSC), and transmission electron microscopy (TEM). In addition, numerical analysis was undertaken to evaluate stress and strain fields near whiskers developed during cooling by the differential thermal contraction between whiskers and matrix.

2. Materials and experimental procedures

The materials used in this study were Al–4 wt % Cu unreinforced and reinforced with 5, 10, 15 wt % SiC whiskers. The chemical composition of the matrix material is given in Table I. The aluminium alloy powders were prepared by inert gas atomization. The SiC whiskers were purchased from Tateho Chemical Co. Japan, which were processed using a pyrolytic process involving silicon and carbon obtained from ground rice hulls. The average dimensions of the whiskers were 0.5 μm diameter and 50 μm long before processing. Gas-atomized 230 mesh Al–4 wt % Cu

TABLE I Chemical composition of the matrix material (wt %)

Cu	Cr	Fe	Mg	Mn	Si	Al
3.98	0.06	0.44	0.08	0.05	0.07	rem.

0022–2461

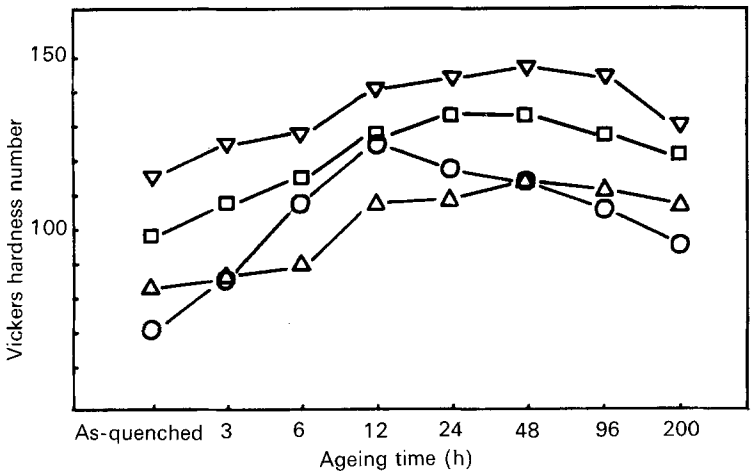

Figure 1 The variation of macrohardness as a function of ageing time for the SiC whisker-reinforced and unreinforced Al–4 wt % Cu aged at 433 K. (○) unreinforced, (△) 5% SiC, (□) 10% SiC, (▽) 15% SiC.

powders were mixed with 5, 10, 15 wt % SiC whiskers dispersed using a supersonic stirrer in buthanol. After 3 h mixing in a rotating mill, the powders blended with SiC whiskers were filtered using an aspirator and dried for 10 h at 463 K in the oven. The powders were then hot pressed at 75 kgf cm^{-2} for 15 min at 863 K. For comparison purposes, a monolithic Al–4 wt % Cu was synthesized identically from the same powder batch. The dimensions of the hot-pressed materials were 40 mm diameter and ~ 30 mm long. The materials, cut in the form of small blocks, were solution treated for 2 h at 793 K, quenched in ice–water and then artificially aged in a silicone oil bath at 433 and 468 K for various times. Because of the possibility of room-temperature ageing, all of the specimens were stored in a freezer after solution treatment and artificial ageing.

Vickers hardness measurements on heat-treated specimens were made using a diamond pyramid indentor and a 5 kgf load. At least six hardness measurements were made for each ageing condition to ensure accurate results. Specimens for DSC analysis were prepared in the form of discs of 5 mm diameter, 0.4 mm thick and were investigated using a heat-compensation type ULVAC DSC 7000 with a plug-in DSC cell. All of the DSC runs began at room temperature, ended at 803 K and were made at a constant heating rate of 5 K min^{-1}. Alumina of approximately equal mass was used as reference material. The specific heat–temperature curve was normalized for the unit mass of metal matrix. TEM specimens were prepared from 0.4 mm thick plate cut using a jeweller's saw and were mechanically polished to a thickness of about 50 μm. Final thinning was carried out using an ion mill, operating at 4 kV, and ion current of 5 to 15 mA and a sample inclination of 15° to the ion beam. The unreinforced materials were thinned in a twin jet polisher with a 10% perchloric acid, 90% methanol using a potential of 25 V at a temperature of about − 25 °C. To investigate the dislocation in the matrix, some of the SiC whisker-reinforced materials were also prepared by the same techniques. The thin foils were examined in detail using Jeol 200CX transmission electron microscopy operating at 160 kV.

3. Experimental results

3.1. Vickers hardness measurements

Fig. 1 shows the variation of macrohardness as a function of ageing times for the whisker-reinforced and unreinforced Al–4 wt % Cu aged at 433 K. As expected, it can be found that the hardness of materials, solution treated and water quenched, increases evenly with the increasing reinforced SiC whisker content. However, there are noticeable differences in age-hardening behaviour between the reinforced and unreinforced materials. Whereas the peak ageing time is about 12 h in the unreinforced material, the whisker-reinforced materials exhibit maximum hardness after 1 to 2 d ageing. Another interesting feature of this figure is the noticeable difference in the magnitude of age hardening. The amount of age hardening is about 30 H_v in the whisker reinforced materials, which is smaller than that in the unreinforced material by 20 H_v. The variation of the peak ageing time as a function of reinforced SiC whisker content was not discernible.

3.2. Calorimetric measurements

Fig. 2 shows the results of the calorimetric measurements as a function of SiC whisker content for the solution-treated and water-quenched materials. The endothermic reaction started at 360 K is due to the reversion of GP zones, which means the formation of a GP zone at below 360 K. The two exothermic reactions, which exhibit peaks at 458 K and 523 K, are due to the precipitation of metastable phases (primarily θ″ and θ′). The endothermic reactions above 600 K are due to the dissolution of θ″, θ′ and the growth of precipitates θ. This precipitation behaviour is modified by the SiC whisker reinforcement as shown in Fig. 2b, c and d. When the material is reinforced with SiC whiskers, it is noticeable that the first exothermic peak decreases as the reinforced SiC whisker content increases. However, a difference in the peak temperature on the DSC curves is not discernible.

The results of DSC measurements on the materials artificially aged for various times are shown in Figs 3 and 4. The exothermic reaction at about 458 K is not

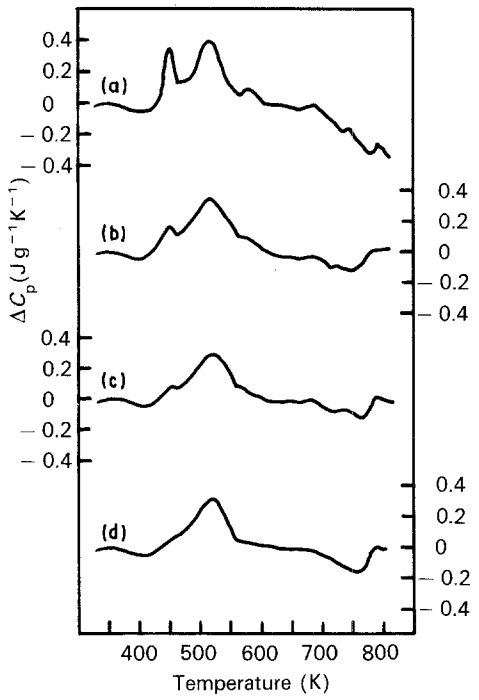

Figure 2 The results of the differential scanning calorimetry for the solution-treated and water-quenched materials. (a) Al–4 wt % Cu; (b) Al–4 wt % Cu, reinforced with 5 wt % SiC whiskers; (c) Al–4 wt % Cu, reinforced with 10 wt % SiC whiskers; (d) Al–4 wt % Cu, reinforced with 15 wt % SiC whiskers.

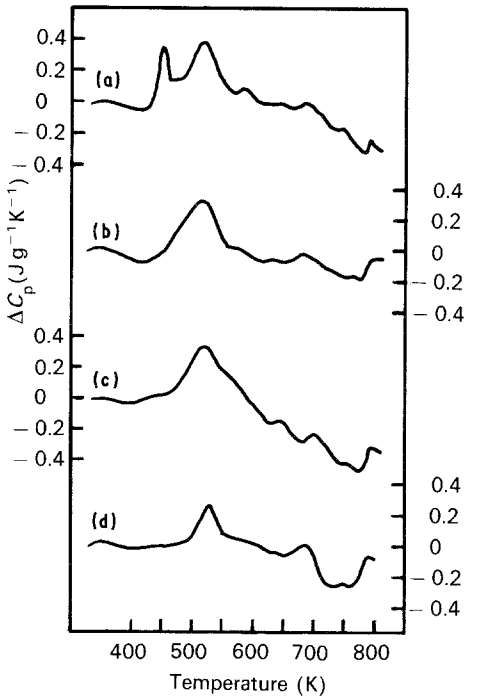

Figure 3 The results of the differential scanning calorimetry for the unreinforced Al–4 wt % Cu, artificially aged at 433 K. (a) As-quenched; (b) aged for 3 h; (c) aged for 6 h; (d) aged for 12 h.

found after 3 h ageing at 433 K (Fig. 3b). The endothermic reaction by the reversion of GP zones almost disappeared after 6 h ageing at 433 K in the unreinforced material (Fig. 3c). In the whisker-reinforced material, this reaction finished earlier than in the unreinforced material (Fig. 4b). After 12 h ageing at 433 K, which corresponds to the peak ageing time for the unreinforced material, the second exothermic peak at 523 K slightly decreases in both materials. This result indicates that the maximum age hardening is obtained by the precipitation of θ″ and θ′ in the unreinforced material, which corresponds to that obtained by the X-ray method [9, 10]. The results of DSC measurements for both the materials aged for over 12 h at 433 K exhibited a similar behaviour (Figs 3d and 4c and d). Notice that the second exothermic peak at 523 K almost disappeared after 2 days ageing at 433 K. It corresponds to the peak ageing time in the whisker-reinforced materials. This indicates that the age hardening is attained by the precipitation of θ′ in the whisker-reinforced material.

3.3. Transmission electron microscopy

Both the whisker-reinforced and unreinforced materials exhibited precipitate-free microstructure in the solution-treated and quenched state as shown in Fig. 5. The density of dislocations is much higher in the matrix of the whisker-reinforced materials than that in the unreinforced material (Fig. 5a and b). The dislocations generated from whiskers are also noticeable as shown in Fig. 5c.

Microstructural developments of the unreinforced material during the artificial ageing are demonstrated in Fig. 6. The densely precipitated θ″ in the matrix and

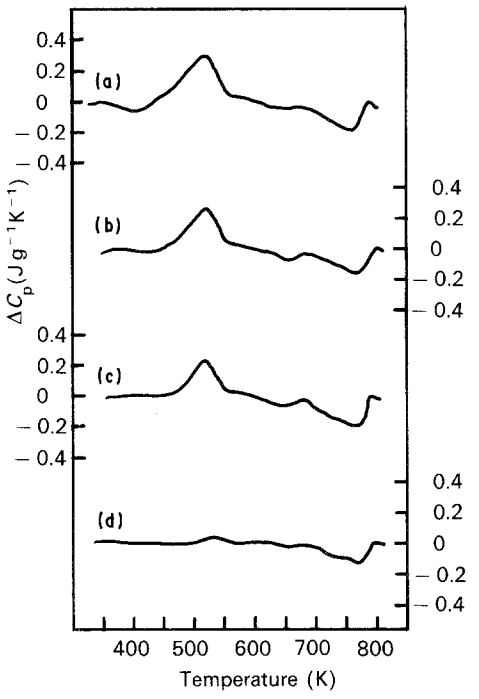

Figure 4 The results of the differential scanning calorimetry for the 15 wt % SiC whisker-reinforced Al–4 wt % Cu, artificially aged at 433 K. (a) As-quenched; (b) aged for 6 h; (c) aged for 12 h; (d) aged for 48 h.

the inhomogeneously precipitated θ on the grain boundary are shown in transmission electron micrographs of the unreinforced material aged for 5 h at 433 K (Fig. 6a). Although inhomogeneously nucleated θ′ on dislocations and θ on grain boundaries were found in the matrix, the magnitude was very small. The microstructure of the unreinforced material aged for 5 h at 468 K consisted of the precipitates θ′ in the matrix and θ on grain boundaries (Fig. 6b).

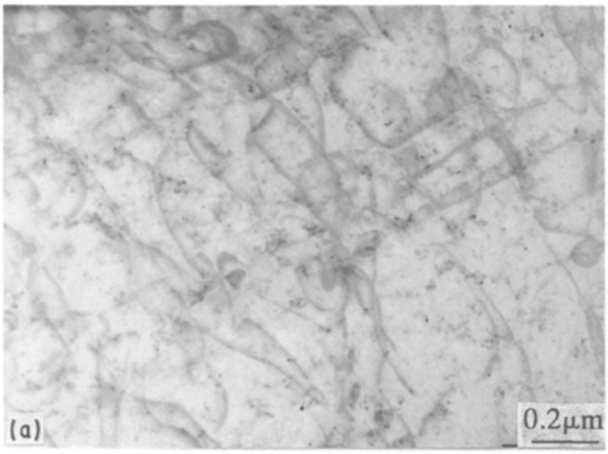

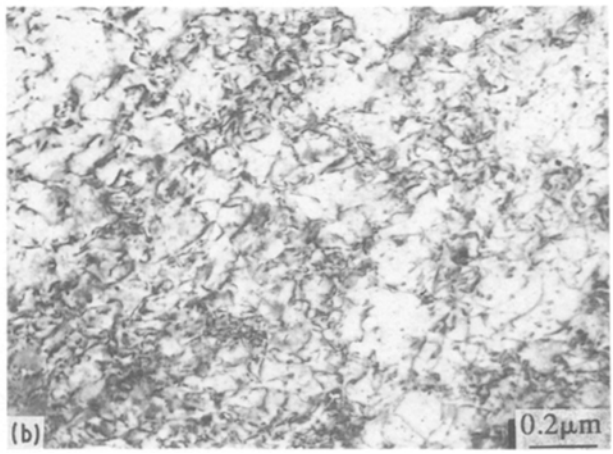

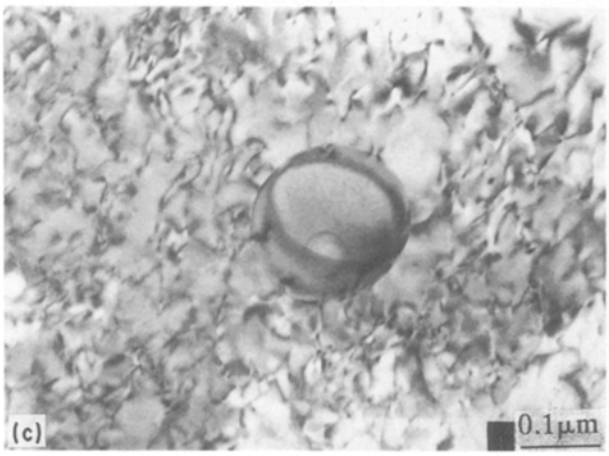

Figure 5 Transmission electron micrographs for the solution-treated and water-quenched materials, which show no precipitates in the matrix. (a) Matrix of the Al–4 wt % Cu; (b) matrix of the 15 wt % SiC whisker-reinforced Al–4 wt % Cu; (c) matrix of the 15 wt % SiC whisker-reinforced Al–4 wt % Cu (dislocations developed from the whisker are shown).

The microstructure of the 15 wt % SiC whisker-reinforced material aged for 5 h at 433 K is shown in Fig. 7. These figures show that the microstructure consisted of the precipitate θ′ in the matrix and θ on grain boundaries. An important feature of this figure is that there does not appear to be θ″ in the matrix (Fig. 7a and b). Although no preferential nucleation of the precipitates near the interface between the whisker and matrix is found, there is some evidence of inhomogeneous nucleation of θ′ (probably on dislocations) in the whisker-rich regions (Fig. 7b).

4. Discussion

4.1. The suppression of θ″ formation in SiC whisker-reinforced Al–Cu alloy

Papazian *et al.* [11] have reported that the precipitation sequence was not affected by SiC reinforcements in the 2124 aluminium alloy but the volume fraction of GPB zones was decreased with increasing SiC reinforcement. They suggested that the decrease in the volume fraction of GPB zones is due to the increased quench sensitivity by SiC reinforcements. In this work, however, we could not find such a quench sensitivity in the SiC whisker-reinforced materials. Transmission electron micrographs showed no precipitates for the SiC whisker-reinforced materials in the solution-treated and quenched state (Fig. 5b, c). No evidence of age hardening for the reinforced material can be seen in the solution-treated and quenched state (Fig. 1).

The present work clearly indicates that the peak ageing time in the whisker-reinforced Al–Cu metal

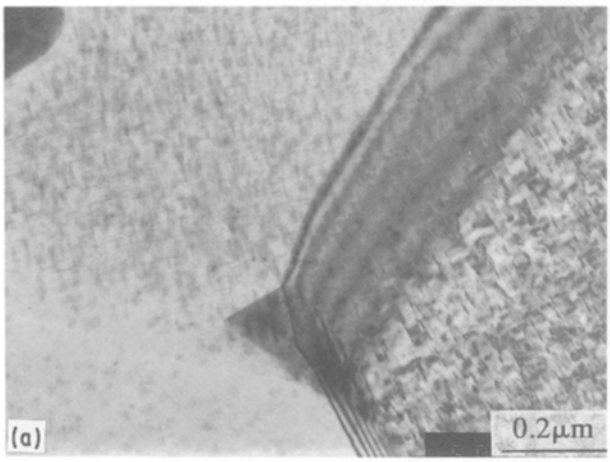

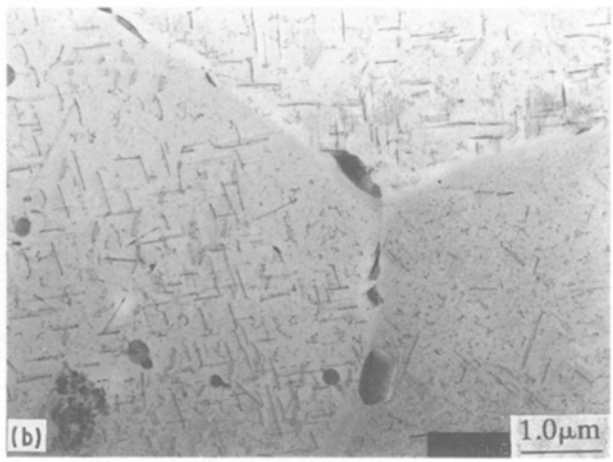

Figure 6 Transmission electron micrographs of the Al–4 wt % Cu, solution treated and artificially aged at various temperatures. (a) Isothermally aged for 5 h at 433 K; (b) isothermally aged for 5 h at 458 K.

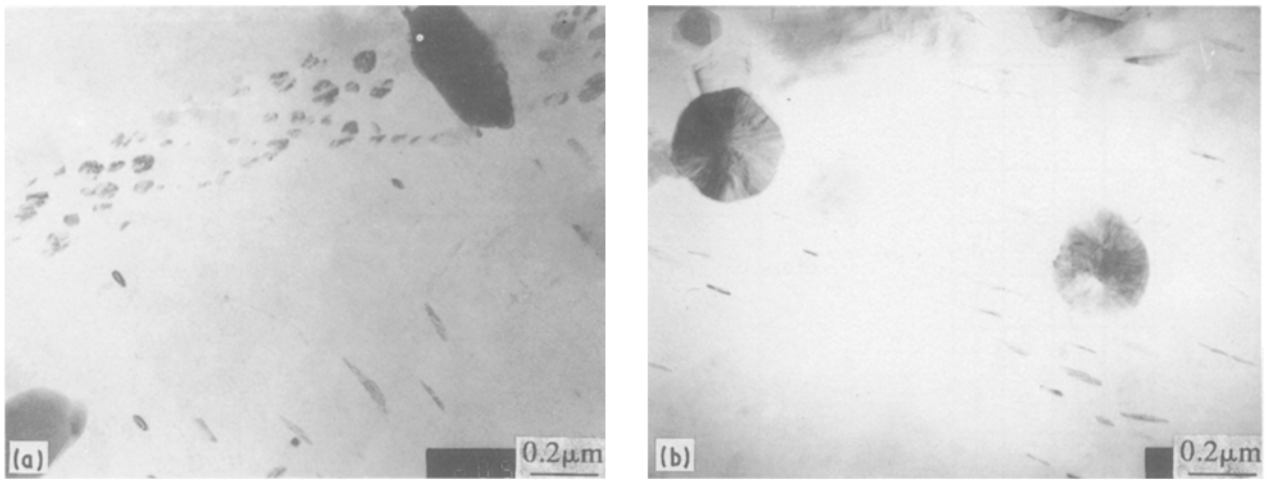

Figure 7 Transmission electron micrographs of the Al–4 wt % Cu, solution treated and artificially aged for 5 h at 433 K. Inhomogeneously nucleated θ′ are shown in the matrix. Notice that θ″ precipitates are not shown in the matrix. (a) θ′ precipitates in the matrix; (b) SiC whisker and θ′ precipitates.

matrix composite is significantly retarded as shown in Fig. 1. Another interesting feature is that the magnitude of hardening by artificial ageing is much smaller in the whisker-reinforced material than that in the unreinforced material. The reason for these features may lie in the differences in the DSC curves and transmission electron micrographs for the reinforced and unreinforced materials. The DSC measurements for solution-treated and quenched materials show that the first exothermic reaction at about 458 K gradually disappears as the content of reinforced whisker increases (Fig. 2). As shown in Fig. 3, the maximum age hardening in the unreinforced material is obtained by the precipitation of the first exothermic phase and the partial precipitation of the second exothermic phase (about 30%). However, the maximum hardening in the whisker-reinforced material is obtained primarily by the precipitation of the second exothermic phase (Fig. 4). Transmission electron micrographs for the materials aged for 5 h at 433 K show such evidence. Whereas θ″ is precipitated densely in the matrix of the unreinforced material, it is not found in the matrix of the whisker-reinforced material (Fig. 7). Through these observations we could conclude that the first exothermic reaction shown in the DSC curve of the unreinforced material is by the precipitation of θ″ and its formation is suppressed by the introduction of SiC whiskers.

The suppression of θ″ precipitation has been reported in the prestrained Al–Cu matrix [12, 13]. Although the reason for this is not yet clear, it was suggested by Graf and Guinier [12] that θ″ could only nucleate on $\{1\,0\,0\}_{Al}$ planes and these are so distorted in the prestrained material that nucleation could not take place. In SiC whisker-reinforced materials, such a high strain could be generated by the differential thermal contraction between the matrix and reinforcement. A rough estimate indicates that the strain between the aluminium metal matrix and the SiC whiskers introduced by water quenching from 793 K is about 1%. The following calculation using finite element methods (FEM) will show that more strain could be generated during cooling.

4.2. Estimation of the misfit strain generated during cooling

Taya and Mori [14] have developed an analytical model to estimate the misfit strain and dislocation punching distance in the metal-matrix composites. The model, which used Eshelby's equivalent inclusion method, focuses on the relief of the residual stress field induced by thermal contraction mismatch through dislocation motion. Although the model could explain the dislocation generation by the relief of the residual stress, the estimate of the residual stress at whisker ends is considered to be low. Through a numerical analysis using a three-dimensional finite element method (FEM) for the discontinuous fibre-reinforced metal matrix composites, Jeong [15] reported a greater stress concentration at whisker ends than by using Eshelby's equivalent methods. In the present work, we estimated the residual stress field and misfit strain induced by the thermal contraction mismatch using FEM. For the purpose of this calculation, an idealized distribution of whiskers was assumed. The parameters appropriate for SiC whisker-reinforced Al–Cu composites, which are used in our calculation, are summarized in Table II.

TABLE II Material properties used in calculation

	Elastic modulus (GPa)	Poisson's ratio	Yield stress (MPa)	Elasto-plastic tangent modulus (GPa)
SiC whisker	580	0.19	–	–
Al–4 wt % Cu	72.4	0.33	350	7.24

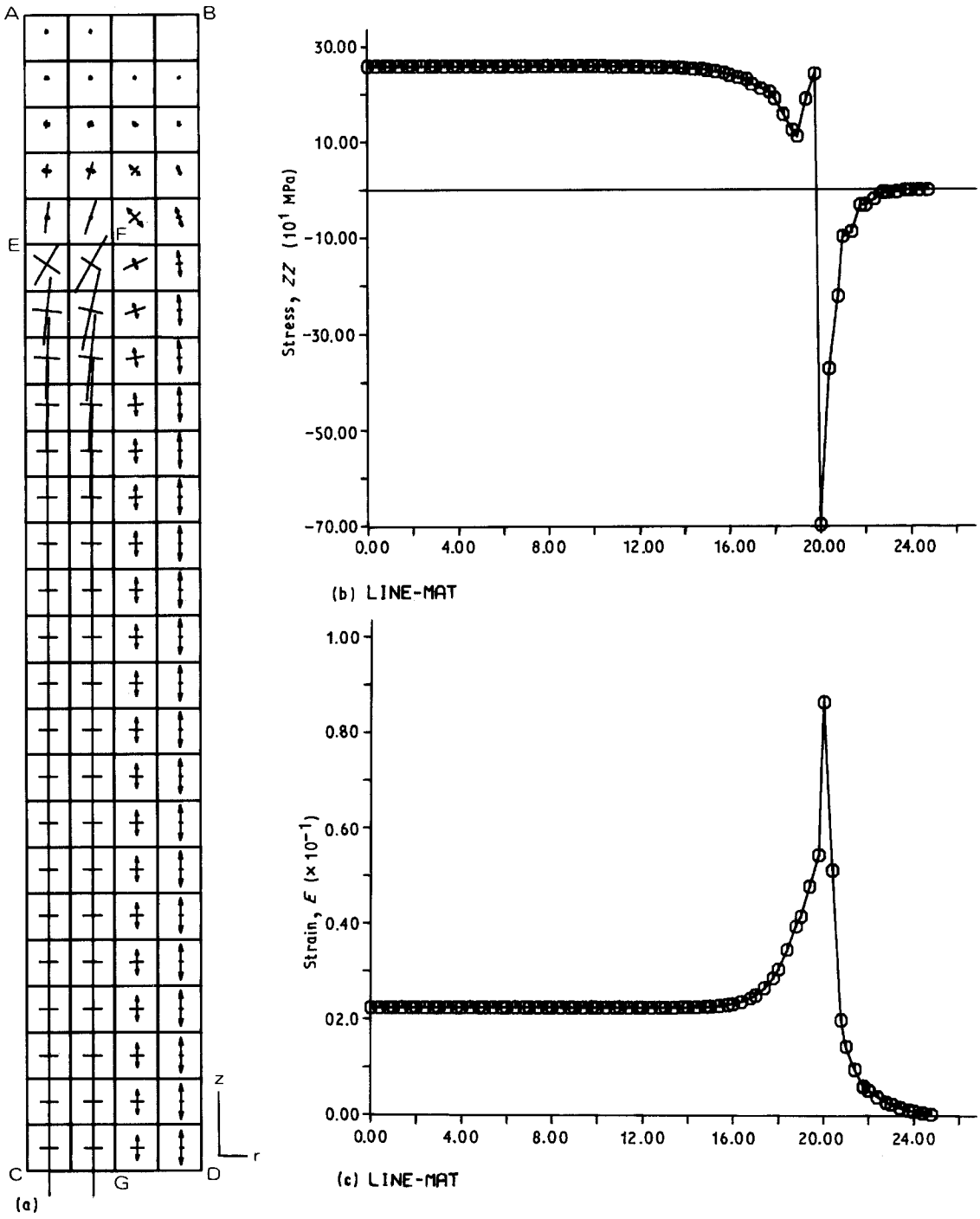

Figure 8 The results of numerical analysis on the misfit stress and strain generated during cooling in the 20 vol % SiC whisker-reinforced Al–4 wt % Cu. (cylindrical model was assumed, EFCG: whisker). (a) Stress field around whisker, the direction and relative magnitude of the principal stress is shown (the line with no arrow means compressive stress and vice versa); (b) stress along the line GF (G: 0.0, F: 20.0); (c) effective strain along the line GF.

The results of our calculation are shown in Fig. 8. They are similar to those of Taya and Mori [14], differing by greater stress concentration near whisker ends. The compressive stress field near whisker ends and the tensile stress field along the whisker–matrix interface are developed during cooling (Fig. 8a). The variation of effective stress and strain along the interface between the matrix and whisker is shown in Fig. 8b and c. The high concentration of stress and strain at whisker ends is noticeable. The effective strain at the interface exceeds the value needed for the plastic deformation of the matrix. Although the density of dislocations generated by the misfit strain could not be estimated in our analysis, the plastic deformation of the matrix near whiskers strongly indicates that there is a high density of dislocations and a strain in the matrix. The stress concentration at whisker ends also suggests that the dislocation is punched out at whisker ends during cooling. The implications of the analysis are supported by experimental observations in this work. Our TEM studies reveal a significantly higher density of dislocations in the matrix of the whisker-reinforced material than that in the unreinforced material (Fig. 5a, b). A high concentration of dislocation lines away from the whisker is also found (Fig. 5c). The experimental evidence and analysis

strongly suggest that the suppression of θ″ formation might be done by a high density of dislocations and a strain generated during cooling.

5. Conclusions

Particular attention was focused on the precipitation characteristics of the SiC whisker-reinforced Al–Cu alloy. An understanding of these phenomena is important in the alteration of matrix properties of aluminium metal–matrix composites. The following conclusions were drawn in this study.

1. The retardation of peak ageing time in the SiC whisker-reinforced Al–Cu alloy was found. However, the variation of the peak ageing time as a function of reinforced SiC whisker content was not discernible. The magnitude of age hardening in SiC whisker-reinforced materials was much smaller than that in the unreinforced material.

2. DSC measurements and transmission electron micrographs for the whisker-reinforced and unreinforced materials revealed that the suppression of θ″ formation by the introduction of SiC whisker reinforcement played an important role in these phenomena.

3. Numerical analysis using FEM was performed to evaluate stress and strain fields developed by the differential thermal contraction between matrix and whiskers during cooling. The results reveal that a high strain at whisker ends is developed and plastic deformation of the matrix near whiskers should occur.

4. Through transmission electron micrographs which exhibited a high density of dislocations in the matrix of whisker-reinforced material, especially near whiskers, we could confirm that such a high strain in the matrix near whiskers is generated during cooling. The suppression of θ″ precipitation in the whisker-reinforced Al–Cu alloys was considered to be the same phenomenon reported in prestrained Al–Cu alloy, which might be done by the suppression of θ″ nucleation on dislocations.

Acknowledgements

The authors thank D. H. Kim for his help with the TEM specimen preparation and M. S. Lee for his assistance with the experiments.

References

1. T. G. NICH and R. F. KARLAK, *Scripta metall.* **18** (1984) 25.
2. T. CHRISTMAN and S. SURESH, *Acta Metall.* **36** (1988) 1691.
3. S. CERESARA and P. FIORINI, *Powder Metall.* **1** (1979) 1.
4. *Idem, ibid.* **4** (1981) 210.
5. C. M. FRIEND and S. D. LUXTON, *J. Mater. Sci.* **23** (1988) 3173.
6. S. R. NUTT and R. W. CARPENTER, *Mater. Sci. Engng* **75** (1985) 169.
7. H. I. LEE *et al.*, KAIST report for project I11610, Korea (1986).
8. H. I. LEE *et al.*, Technical report MARD-411-88099, Korea (1988).
9. J. M. SILCOCK, T. J. HEAL and H. K. HARDY, *J. Inst. Metals* **82** (1953–1954) 239.
10. H. K. HARDY, *ibid.* **79** (1951) 321.
11. J. M. PAPAZIAN, A.LEVY and P. N. ALDER, Technical report AFOSR-TR-87-1658, USA (1987).
12. R. GRAF and A. GUINIER, *Compt. Rend.* **238** (1954) 2175.
13. J. D. COOK and J. NUTTING, in "The mechanism of phase transformation in crystalline solids," edited by R. B. Nicholson (The Institute of Metals, London, 1968) p. 54.
14. M. TAYA and T. MORI, *Acta Metall.* **35** (1987) 155.
15. I. B. JEONG, PhD thesis, Seoul National University, Korea (1988).

Received 1 March
and accepted 30 August 1989